International Journal of Innovative Computing, Information and Control
Volume **19**, Number **6**, December **2023**
 ISSN 1349-4198
pp. **1735–1751**

HIERARCHICAL DISTRIBUTED MODEL PREDICTIVE CONTROL FOR MULTIPLE HYBRID ENERGY STORAGE SYSTEMS IN A DC MICROGRID

Weilin Yang, Chaonan Zhao, Guanyang Hu, Dezhi Xu* and Tinglong Pan

School of Internet of Things Engineering
Jiangnan University
No. 1800, Lihu Avenue, Wuxi 214122, P. R. China
{ wlyang; tlpan }@jiangnan.edu.cn; { 6201925031; guanyanghu }@stu.jiangnan.edu.cn
*Corresponding author: xudezhi@jiangnan.edu.cn

Received February 2023; revised May 2023

Abstract. *The coordination and optimization between multiple hybrid energy storage systems in direct current (DC) microgrid can effectively meet the load demand of microgrid and extend the life of generator sets, thus ensuring the stability and safety of grid operation. In this paper, a hierarchical distributed model predictive control is constructed; the upper layer employs an iterative distributed control strategy for the purpose of power scheduling coordination, while the lower layer uses finite-control set model predictive control to achieve accurate power tracking. The optimization problem in the upper layer is solved by the alternating direction method of multipliers. Moreover, the time delay caused by computations is taken into account by considering one-step delay compensation. Simulations show the effectiveness of the proposed method in hybrid energy storage system control.*
Keywords: DC microgrid, Hybrid energy storage system, Distributed model predictive control

1. **Introduction.** A direct current (DC) microgrid is a power generation system that effectively integrates various generation resources, loads, and energy storage elements into a single information network [1-3]. In DC microgrids, energy storage systems can guarantee the continuous supply of electrical energy and store excess power to improve the power quality [4,5]. The hybrid energy storage system (HESS) technologies, compared to individual energy storage systems, have complementary characteristics in several aspects such as power, energy dense and life cycle, which can better achieve the required energy storage purpose [6-8]. However, configuration and control issues associated with HESS need to be addressed [9-11].

Hybrid energy storage technology plays an important role in improving the efficiency of DC microgrid operation as a means to optimize the allocation of energy [12,13]. [14] used prescribed performance control for an HESS for an electric vehicle system to achieve the system steady-state response. [15] showed the distribution of high and low frequency power fluctuations of an HESS through a low-pass filter. [16] developed a controller based on the MPC approach to efficiently distribute variable power loads and renewable energy generation into two different energy storage devices in the converter. [17] used dynamic programming to handle the optimization problem to obtain the optimal configuration and energy allocation strategy for the HESS.

DOI: 10.24507/ijicic.19.06.1735

However, with the increasing scale of microgrids, the above methods have become difficult to meet the demand in the face of multiple hybrid energy storage devices, and it has been proposed to achieve overall control of microgrids by layering them into control [18,19]. Typically, the upper layer operates optimally based on nonlinear models related to grid safety and economic standards, such as voltage security and economical dispatch strategy [20-22]. The goal of this layer is to coordinate power distribution in a hybrid system to keep the grid balanced while reducing overall operating costs. The lower level involves precise tracking control over the upper level settings [23]. Therefore, the energy management strategy coordinates the power allocation of each hybrid storage unit at the upper layer to provide the required power to the system, where the power allocation can be based on the SOC of each hybrid storage device to extend the lifetime or energy prediction based on the dynamic environmental information on the energy consumption side [24,25]. The power regulation of each unit is implemented in the lower layer. A multilayer distributed model predictive control (DMPC) strategy based on voltage observer is proposed in [26], which achieves a compromise between voltage regulation as well as power sharing and reduces the impact of communication delays, but it does not take into account the HESS in DC microgrids. Therefore, this paper proposes a DMPC-based coordination control scheme for multiple HESSs in DC microgrids.

In the DC microgrid system, the generator and energy storage device are connected to the DC bus through converters [27-29]. Designing efficient controllers for power converters has become one of the research hotspots of scholars. Model predictive control (MPC) is widely used because it has the advantage of systematically dealing with multiple objectives and constraints [30]. [31] established a DC microgrid model with multiple buses, realizing proportional current sharing and voltage balance. Because of its fast dynamic response, high current control performance and ability to handle multiple constraints, [32] used finite control set model predictive control (FCS-MPC) in motor control. [33] proposed to apply FCS-MPC to power converter and compared it with traditional control technology. [34] applied FCS-MPC to HESS to keep the voltage and current of the hybrid energy storage unit within a predetermined range. However, it is difficult to expand into multiple HESSs because of the heavy computational burden involving multiple matrix operations and the huge computational resources and memory required for the controller and the centralized control method is not suitable for the control problem of multiple HESSs. Therefore, FCS-MPC is used in this paper for the tracking control of a single HESS in the lower layer, and the upper layer of the distributed control method is used to solve the coordinated control problem of multiple HESSs.

In this paper, an effective hierarchical distributed model predictive control (HDMPC) method is proposed for a DC microgrid with multiple hybrid energy storage systems. The energy management system (EMS) in the upper layer constructs a cost function for the economy and safety of the HESS, solves the optimization problem using the alternating direction multiplier algorithm (ADMM) to achieve optimal coordination of power distribution. And the lower layer achieves optimal coordination of power distribution through the FCS-MPC to achieve the tracking output of the optimal power value given by the upper layer.

The paper is organized as follows. HESS is modeled in Section 2. Section 3 presents the strategy of HDMPC and proposes an optimization scheme for the actual operation problem. The simulation software is used in Section 4, and its simulation results verify that the performance of the proposed control strategy is better than that of the conventional control method. Finally, Section 5 concludes the study.

2. **System Description.** The topology structure of the DC microgrid system is shown in Figure 1, which consists of a generator set and multiple HESSs. The HESS can provide power when the generator set cannot meet the load demand. Energy is collected by the DC bus from the generator set, each storage unit, and then transferred to the load. In order to achieve efficient and economical power distribution, the dynamic performance of each subsystem must be modeled. When distributed control is used, all energy storage devices exchange status information through communication lines for global coordinated control. Compared with alternating current microgrid, DC microgrid does not need to consider frequency, system synchronization and reactive power. It has the advantages of simple control, safety and stability, high operational efficiency and expandability. In the context of the massive grid connection of distributed DC power sources and the gradually increasing proportion of DC loads, DC microgrids have a very broad development prospect.

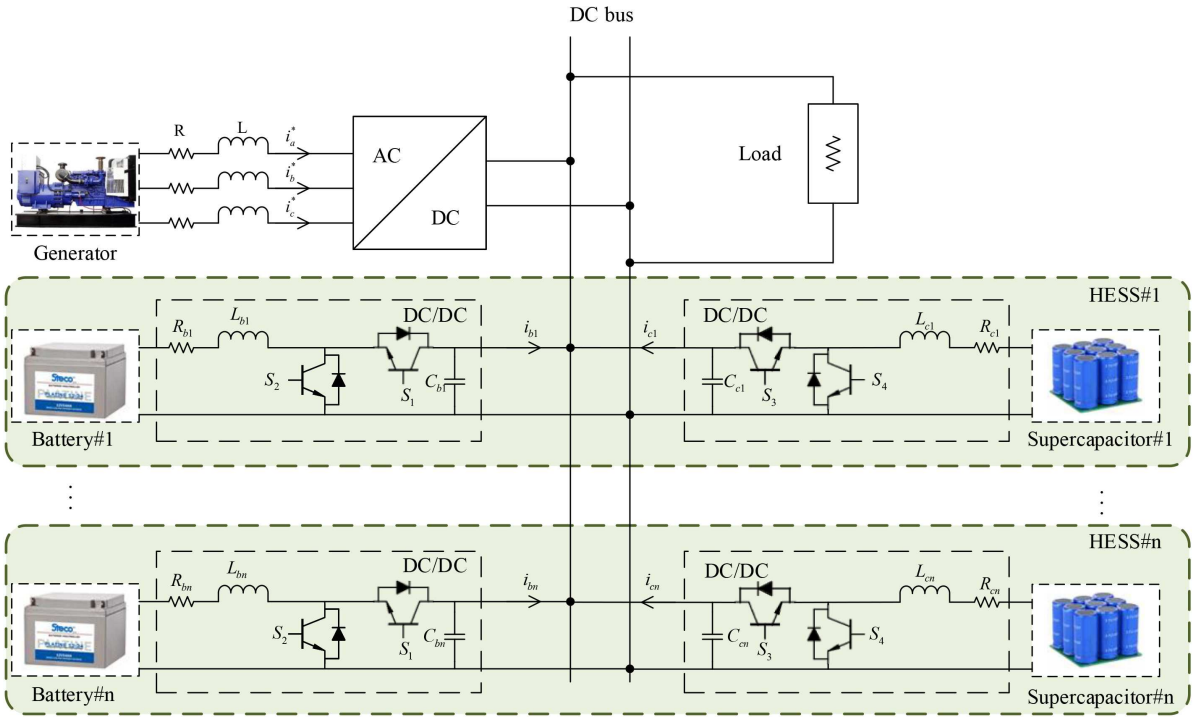

FIGURE 1. The basic topology of the DC microgrid

As shown in Figure 1, all components work in the ideal state, without considering other losses and battery#i and supercapacitor#i indicate the i-th battery and supercapacitor, respectively. R and L are the equivalent resistance and equivalent inductance of the generator, i_a^*, i_b^*, i_c^* are the three-phase current output by the generator. R_{bi} and L_{bi} are the equivalent resistance and equivalent inductance of the battery#i, R_{ci} and L_{ci} are the equivalent resistance and equivalent inductance of the supercapacitor#i, C_{bi} and C_{ci} are the filter capacitor of bidirectional DC/DC converter. S_1, S_2, S_3 and S_4 indicate the working status of four switch tubes in each HESS. $S = 0$ indicates switching tube is off. Conversely, $S = 1$ indicates that the switch is on.

2.1. **Mathematical modeling of the HESS.** Battery is widely used in hybrid energy storage systems. Since both overcharging and deep discharging reduce the battery life, it is necessary to keep the state of charge of the battery in a certain range. The discrete-time dynamic SOC model of a battery in the HESS has the following form:

$$q_b(k+1) = q_b(k) - \frac{\eta_b \Delta t}{Q_N U_b} P_b(k) \tag{1}$$
$$\text{s.t. } q_{\min,b} \le q_b \le q_{\max,b}$$

where η_b is the coefficient of battery charge/discharge efficiency, Δt is the sample time in EMS layer (will be use), Q_N is the rated capacity of battery, U_b is the battery voltage, $P_b(k)$ is the power injected into the DC bus by the battery at the time k, $q_{\min,b}$ and $q_{\max,b}$ are the lower, and upper limits of the battery SOC, respectively.

Because supercapacitors and batteries are also voltage source devices, the EMS-layer SOC model of supercapacitors can be expressed in a similar way:

$$q_c(k+1) = q_c(k) - \frac{\eta_c \Delta t}{Q_N U_c} P_c(k) \tag{2}$$
$$\text{s.t. } q_{\min,c} \le q_c \le q_{\max,c}$$

where η_c is the coefficient of supercapacitors charge/discharge efficiency, U_c is the battery voltage, $P_c(k)$ is the power injected into the DC bus by the supercapacitors at the time k, $q_{\min,c}$ and $q_{\max,c}$ are the lower, and upper limits of the capacitor SOC, respectively.

As an energy storage unit in DC microgrid, the battery is cyclically charged and discharged. Since the battery voltage is different from the DC bus voltage level, a bidirectional DC/DC converter is needed to complete the voltage conversion and energy transfer tasks. Supercapacitors also transfer energy to DC microgrid through DC/DC converters, so the mathematical model of supercapacitor is the similar as the mathematical model of battery. There are two modes of its operation as follows.

When the battery and supercapacitor are discharged, the energy is transferred to the DC bus through the converter. Since the terminal voltage of the battery is lower than the DC bus, the converter works in boost mode. The discrete-time state-space model is obtained as

$$\begin{cases} P_{bi}^{\text{ref}} > 0 \\ i_{bi}(k+1) = \left(1 - \dfrac{TR_{bi}}{L_{bi}}\right) i_{bi}(k) + \dfrac{T}{L_{bi}} U_{bi}(k) - \dfrac{1-S_2}{L_{bi}} U_{dc}(k) \\ U_{dc}(k+1) = \dfrac{T(1-S_2)}{C_{bi}} i_{bi}(k) + \left(1 - \dfrac{T}{R_{bi}C_{bi}}\right) U_{dc}(k) \end{cases} \tag{3}$$

$$\begin{cases} P_{ci}^{\text{ref}} > 0 \\ i_{ci}(k+1) = \left(1 - \dfrac{TR_{ci}}{L_{ci}}\right) i_{ci}(k) + \dfrac{T}{L_{ci}} U_{ci}(k) - \dfrac{1-S_4}{L_{ci}} U_{dc}(k) \\ U_{dc}(k+1) = \dfrac{T(1-S_4)}{C_{ci}} i_{ci}(k) + \left(1 - \dfrac{T}{R_{ci}C_{ci}}\right) U_{dc}(k) \end{cases} \tag{4}$$

where P_{bi}^{ref} and P_{ci}^{ref} are the power reference value of the battery and supercapacitor, i_{bi} and i_{ci} are the working current of the battery and supercapacitor, U_{bi} and U_{ci} are the working voltage of the battery and supercapacitor, U_{dc} is DC bus voltage and T is the sample time in power tracking layer.

Conversely, when the battery and supercapacitor are charging, the converter operates in buck mode and the energy is transferred from the DC bus to the battery:

$$\begin{cases} P_{bi}^{\text{ref}} < 0 \\ i_{bi}(k+1) = \left(1 + \dfrac{TR_{bi}}{L_{bi}}\right) i_{bi}(k) - \dfrac{TS_1}{L_{bi}} U_{bi}(k) + \dfrac{1}{L_{bi}} U_{dc}(k) \\ U_{dc}(k+1) = -\dfrac{TS_1}{C_{bi}} i_{bi}(k) + \left(1 - \dfrac{T}{R_{bi}C_{bi}}\right) U_{dc}(k) \end{cases} \tag{5}$$

$$\begin{cases} P_{ci}^{\text{ref}} < 0 \\ i_{ci}(k+1) = \left(1 + \dfrac{TR_{ci}}{L_{ci}}\right) i_{ci}(k) - \dfrac{TS_3}{L_{ci}} U_{ci}(k) + \dfrac{1}{L_{ci}} U_{dc}(k) \\ U_{dc}(k+1) = -\dfrac{TS_3}{C_{ci}} i_{ci}(k) + \left(1 - \dfrac{T}{R_{ci}C_{ci}}\right) U_{dc}(k) \end{cases} \tag{6}$$

2.2. **Power distribution strategy.** When more rapid load fluctuations are generated, the generation equipment in the microgrid is not sufficient to maintain the balance between the supply side and the load side due to its own physical constraints, resulting in bus voltage fluctuations. Therefore, some of this shortfall power needs to be allocated to the HESS to make up for the shortfall in system output. The power allocation strategy for this part is as follows.

First, at the sampling time k, the rate of change ΔP_g of the current load demand P_l with respect to the generator output at the previous sampling moment $P_g(k-1)$ is calculated:

$$\Delta P_g = (P_l - P_g(k-1))/\Delta t \tag{7}$$

where Δt is the sample time.

Next, the following two cases are set according to the load change rate ΔP_g and the maximum climbing power of the generator P_g^{climb}.

Case 1: $\Delta P_g \leq P_g^{\text{climb}}$ when the load demand change rate does not exceed the climbing power of the generator, the load power is output by the generator, and the power commands as follows:

$$P_g(k) = P_l(k), \quad P_{\text{HESS}} = 0 \tag{8}$$

Case 2: $\Delta P_g > P_g^{\text{climb}}$ when the change rate of load demand exceeds the climbing power of the generator, the HESS will output the excess power P_{HESS}.

$$P_g(k) = P_g(k-1) + \text{sign}(\Delta P_g) P_g^{\text{climb}} \Delta t \tag{9}$$

$$P_{\text{HESS}}(k) = P_l(k) - P_g(k) \tag{10}$$

The system description in the above allows us to build an accurate dynamics model of the DC microgrid system, which is the necessary foundation for the subsequent design of the HDMPC strategy.

3. **The HDMPC Strategy.** The scheme of HDMPC for hybrid energy storage power generation system is shown in Figure 2. The distributed model predictive controller is designed to coordinate the power distribution between each hybrid energy storage unit to meet the load demand in the upper layer. And the model prediction controller based on the dynamic model of each distributed hybrid energy storage unit is designed in the lower layer to accurately track the control set in the upper layer. EMS-layer DMPC gets the reference power calculated by the other distributed unit from the communication network and provides reference power for each distributed unit based on its SOC level, generated by an objective function that incorporates economic and safety standards, it aims to reduce overall operating costs and achieve flexibility in each unit while maintaining the stability of the hybrid system. The reference power of each HESS obtained from the upper

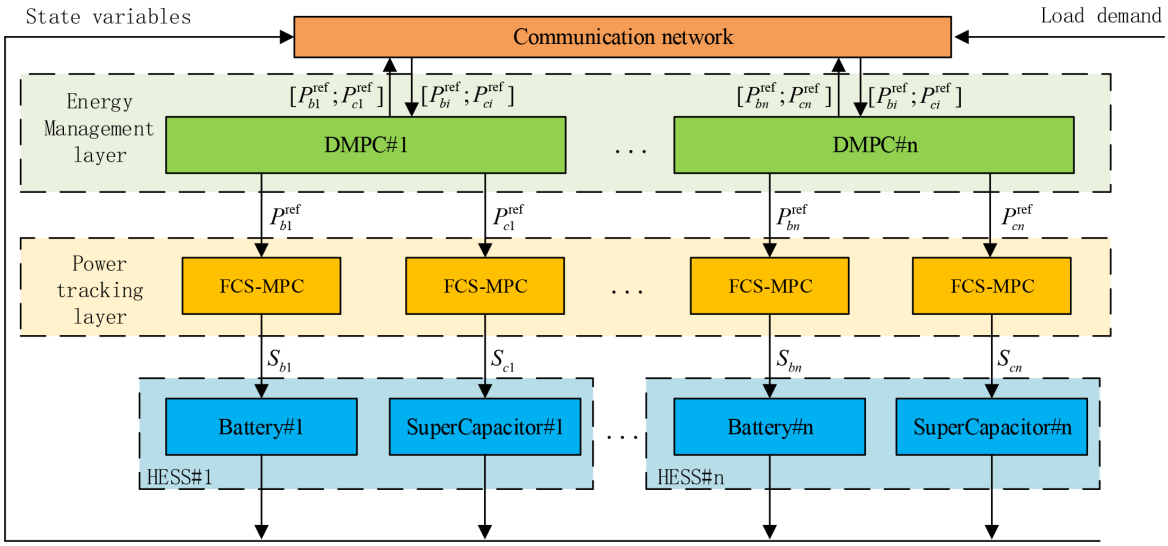

FIGURE 2. Control structure of the HDMPC

layer is transmitted to the lower layer. In the lower layer, the FCS-MPC at the power tracking layer provides the optimal switching sequence generated by the tracking objective function directly to the switching tubes, eliminating the need for the pulse modulation module. The switching tubes directly control each hybrid energy storage unit.

3.1. **EMS-layer DMPC.** The main task of EMS is to ensure safe and reliable operation of DC microgrid by maintaining a balance between power supply and load demand. To improve the operating economy, high SOC levels are given priority, and low SOC levels will reduce their part in the power distribution. Therefore, the cost function at the EMS layer can be expressed as

$$J(k) = J_1(k) + J_2(k) + J_3(k) \tag{11}$$

$$J_1(k) = \sum_{j=1}^{N} \left\| P_{\text{HESS}}(k+j|k) - \sum_{i=1}^{n} P_{bi}(k+j|k) - \sum_{i=1}^{n} P_{ci}(k+j|k) \right\|_{Q_1}^2$$

$$J_2(k) = \sum_{j=1}^{N} \sum_{i=1}^{n} \|q_{bi}(k+j|k) - \bar{q}_b\|_{Q_2}^2$$

$$J_3(k) = \sum_{j=1}^{N} \sum_{i=1}^{n} \|q_{ci}(k+j|k) - \bar{q}_c\|_{Q_3}^2$$

$$\text{s.t. } (1), (2)$$

where J_1 indicates the safety and reliability of the HESS, J_2 indicates the cost of battery, J_3 indicates the cost of supercapacitor, Q_1, Q_2 and Q_3 are weight matrices that are postive definite which satisfies $\|Z\|_Q^2 = Z^T Q Z$, $P(k+j|k)$ and $q(k+j|k)$ are the predicted values at $k+j$ with given current energy storage units informations at k and N is the prediction horizon.

Thus, the corresponding optimization problems to be solved at the EMS layer is

$$\left[P_{bi}^{\text{ref}}; P_{ci}^{\text{ref}}\right]^* = \arg \min_{\left[P_{bi}^{\text{ref}}; P_{ci}^{\text{ref}}\right]} J(k) \tag{12}$$

where

$$\left[P_{bi}^{\mathrm{ref}}; P_{ci}^{\mathrm{ref}}\right]^{*} = \begin{bmatrix} P_{b1}^{\mathrm{ref}}(k) & P_{b1}^{\mathrm{ref}}(k+1|k) & \cdots & P_{b1}^{\mathrm{ref}}(k+N-1|k) \\ \cdots & \cdots & \cdots & \cdots \\ P_{bi}^{\mathrm{ref}}(k) & P_{bi}^{\mathrm{ref}}(k+1|k) & \cdots & P_{bi}^{\mathrm{ref}}(k+N-1|k) \\ \cdots & \cdots & \cdots & \cdots \\ P_{bn}^{\mathrm{ref}}(k) & P_{bn}^{\mathrm{ref}}(k+1|k) & \cdots & P_{bn}^{\mathrm{ref}}(k+N-1|k) \\ P_{c1}^{\mathrm{ref}}(k) & P_{c1}^{\mathrm{ref}}(k+1|k) & \cdots & P_{c1}^{\mathrm{ref}}(k+N-1|k) \\ \cdots & \cdots & \cdots & \cdots \\ P_{ci}^{\mathrm{ref}}(k) & P_{ci}^{\mathrm{ref}}(k+1|k) & \cdots & P_{ci}^{\mathrm{ref}}(k+N-1|k) \\ \cdots & \cdots & \cdots & \cdots \\ P_{cn}^{\mathrm{ref}}(k) & P_{cn}^{\mathrm{ref}}(k+1|k) & \cdots & P_{cn}^{\mathrm{ref}}(k+N-1|k) \end{bmatrix}$$

are the solution result of the optimal sequence.

The distributed optimization problem shown above is solved using ADMM [35], which employs the following Lagrangian

$$L_{\rho}(x, z, u) = f(x) + g(z) + (\rho/2)\left\|x - z + u\right\|_2^2 \tag{13}$$

where $\rho > 0$ and $u = (1/\rho)y$ is the scaled dual variable.

The detailed procedure is given in Algorithm 1.

Algorithm 1: HDMPC with ADMM algorithm

At the sampling time k

1: Initialize the optimal variables $\left[P_{bi}^{\mathrm{ref}}; P_{ci}^{\mathrm{ref}}\right]^{(0)}$ for each unit. Given the load demand P_{HESS}, number of iterations $l \leftarrow 1$, the maximum iterations $m_{\max}$ and the stopping criteria ϵ^{pri} and ϵ^{dual}.

2: Transmit $\left[P_{bi}^{\mathrm{ref}}; P_{ci}^{\mathrm{ref}}\right]^{(l-1)}$ to all the interconnected unit.

For $\boldsymbol{i = 1, \ldots, n}$ **do**

3: Rewrite (11) as a quadratic program:
$f(x) = 1/2x^T Px + q^T x$
s.t. $lb \leq x \leq ub$
where lb, ub are vectors and $x = \left[P_{bi}^{\mathrm{ref}}; P_{ci}^{\mathrm{ref}}\right]^{(l-1)}$.

4: Express it in ADMM form as:
minimize $f(x) + g(z)$
s.t. $x - z = 0$

5: The scaled form of ADMM consists of the iterations
$x^{l+1} := \arg\min_x \left(f(x) + (\rho/2)\left\|x - z^l + u^l\right\|_2^2\right)$
$z^{l+1} := \left(x^{l+1} + u^l\right)$
$u^{l+1} := u^l + x^{l+1} - z^{l+1}$

End for

6: Compute the primal and dual residuals r^l and s^l

While $\left\|r^l\right\|_2 \geq \epsilon^{\mathrm{pri}}$ **and** $\left\|s^l\right\|_2 \geq \epsilon^{\mathrm{dual}}$ **do**

7: $l + 1 \leftarrow l$ and repeat steps 2 to 6

8: break if $l = m_{\max}$

End while

The algorithm shows that the optimization problem (11) is divided into n subsystems under the distributed control structure. Each energy storage unit computes its own original and dual variables locally using the ADMM algorithm and derives its own optimal solution. Then it exchanges its own information and sends updates with each of the remaining units through the commutation network shown in Figure 2 until the solution reaches

the stopping condition or certain maximum ADMM iterations $m_{\max}$ are reached. Under this distributed control structure, the local optimal solution in each local MPC moves to the global optimal through the iterative process of mutual communication.

The control system using MPC schemes usually cause delays during the implementation due to the heavy computations in the receding horizon optimizations. Therefore, delay compensation should be considered to improve the closed-loop control performance. To this end, we can obtain the power reference of time $k+1$ at time k, i.e., employ one-step delay compensation. Accordingly, Equation (12) is modified as

$$\left[P_{bi}^{\text{ref}}; P_{ci}^{\text{ref}}\right]^* = \arg \min_{\left[P_{bi}^{\text{ref}}; P_{ci}^{\text{ref}}\right]} J(k+1|k) \tag{14}$$

where

$$\left[P_{bi}^{\text{ref}}; P_{ci}^{\text{ref}}\right]^* = \begin{bmatrix} P_{b1}^{\text{ref}}(k|k-1) & P_{b1}^{\text{ref}}(k+1|k) & \cdots & P_{b1}^{\text{ref}}(k+N-1|k) \\ \cdots & \cdots & \cdots & \cdots \\ P_{bi}^{\text{ref}}(k|k-1) & P_{bi}^{\text{ref}}(k+1|k) & \cdots & P_{bi}^{\text{ref}}(k+N-1|k) \\ \cdots & \cdots & \cdots & \cdots \\ P_{bn}^{\text{ref}}(k|k-1) & P_{bn}^{\text{ref}}(k+1|k) & \cdots & P_{bn}^{\text{ref}}(k+N-1|k) \\ P_{c1}^{\text{ref}}(k|k-1) & P_{c1}^{\text{ref}}(k+1|k) & \cdots & P_{c1}^{\text{ref}}(k+N-1|k) \\ \cdots & \cdots & \cdots & \cdots \\ P_{ci}^{\text{ref}}(k|k-1) & P_{ci}^{\text{ref}}(k+1|k) & \cdots & P_{ci}^{\text{ref}}(k+N-1|k) \\ \cdots & \cdots & \cdots & \cdots \\ P_{cn}^{\text{ref}}(k|k-1) & P_{cn}^{\text{ref}}(k+1|k) & \cdots & P_{cn}^{\text{ref}}(k+N-1|k) \end{bmatrix}$$

are the solution result of the optimal sequence.

3.2. **Power tracking layer.** The optimization problem in the lower layer for the i-th HESS unit involves the optimization of both the supercapacitors and batteries. Specifically, the controller in the lower layer tracks the reference signals generated by the upper layer. In this work, FCS-MPC is considered to address the lower layer control problem. Since power converters have a finite number of switching states, the optimization problem can be simplified and reduced to a prediction of the system behavior for only those possible switching states. Each prediction is then used to evaluate the cost function and therefore to select and generate the state with the minimum cost. Taking the battery control as an example, the corresponding optimization problem to be solved is

$$\begin{aligned} &\arg \min_{s(k)} f_{bj} := \left[i_{bi}(k+1) - P_{bi}^{\text{ref}}/U_{bi}\right]^2 + \lambda_b \left[U_{dc}(k+1) - U_{dc}^{\text{ref}}\right]^2 \\ &\text{s.t. } (3), (5) \end{aligned} \tag{15}$$

where $s(k) := [S_1 \ S_2]^T$ is the working status of two switch tubes in the converter, λ_b is a weight matrix, and $j = (1, 2, 3, 4)$. The cost function values of the HESS can be obtained for different switching states in boost mode. Similarly, two different cost function values can be obtained for the buck mode. f_{b1} represents $S_1 = 0$ and $S_2 = 1$, f_{b2} represents $S_1 = 1$ and $S_2 = 0$, f_{b3} represents $S_1 = 1$ and $S_2 = 0$, f_{b4} represents $S_1 = 0$ and $S_2 = 1$. The four different values represent the different working states of the switching tubes. By comparing the magnitude of the different cost function values, the smallest value can be obtained, and the switching state of the switching tube represented by this value is taken as the state output of the next moment. The above process for the supercapacitor control is similar. Thus, it is omitted for brevity.

4. **Simulation Results.** In order to verify the effectiveness and superiority of the proposed HDMPC applied to multiple HESS in this paper, in this section, the control effect of the algorithm is verified by simulation tests. The HESS in Figure 1 is composed of two batteries and two supercapacitors ($n = 2$), and their SOC initial values are set to 60% and 80%, respectively. In the HDMPC, sampling time is set to be $\Delta t = 10$ ms in the EMS layer, and $T = 10$ μs in power tracking layer. Set the predictive and the control horizon both to be $N = 10$. The parameters of each energy storage module are shown in the following Table 1.

TABLE 1. DC microgrid system parameters

Parameter	Value	Parameter	Value
Resistance R	5 mΩ	Battery capacity	50 Ah
Inductance L	30 mH	Battery voltage	500 V
Resistance R_{bi}, R_{ci}	5 mΩ	Supercapacitor capacity	100 F
Inductance L_{bi}, L_{ci}	6 mH	Supercapacitor voltage	500 V
Capacitance C_{bi}	560 μF	Charge/discharge efficiency η_b, η_c	0.92
Capacitance C_{ci}	1000 μF	Maximum climbing power P_g^{climb}	100 kW/min

The power requirement of load is shown in Figure 3. The load on the DC bus is divided between the generator and the HESS and the results are shown in Figure 4. Then set the rated voltage of DC bus $U_{dc}^{\text{ref}} = 800$ V, the referencec SOC $\bar{q}_b = \bar{q}_c = 0.8$ and $q_{\min,b} = q_{\min,c} = 0.2$, $q_{\max,b} = q_{\max,c} = 0.8$. In order to realize the stability of DC bus voltage and control the output reference power of DC microgrid, the simulation is carried out. The feasibility and superiority of the HDMPC control scheme are shown in Figure 5, Figure 6 and Figure 7.

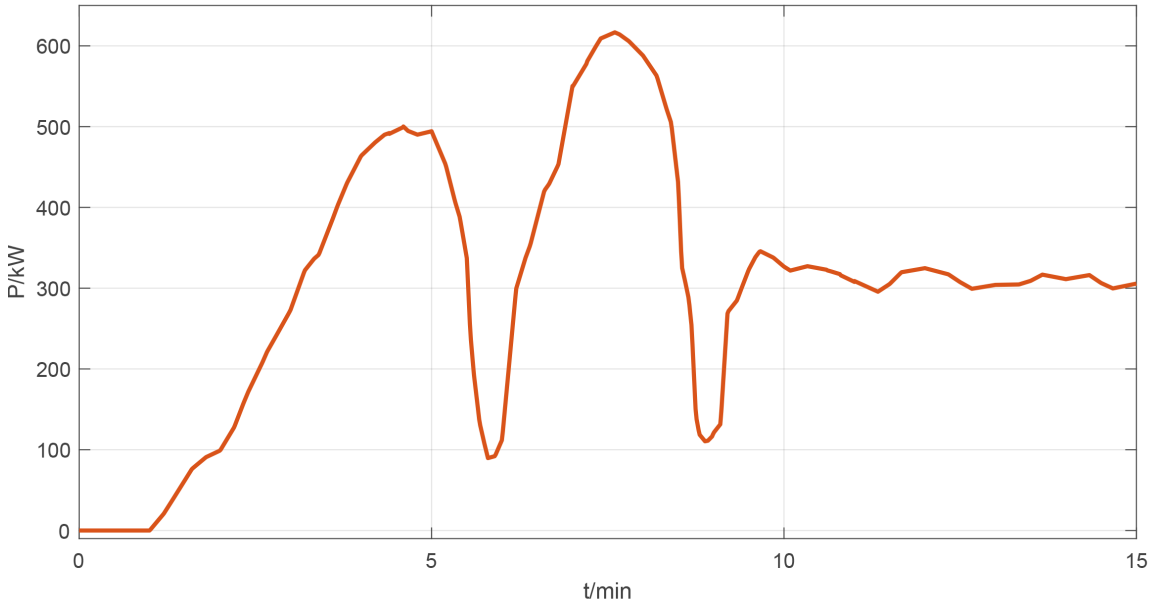

FIGURE 3. The power requirement of load curve

Specifically, Figure 5 shows the DC bus voltage. For comparing purpose, PI and hierarchical centralized MPC (HCMPC) are also constituted, HCMPC uses a centralized MPC at the EMS layer and the same FCS-MPC as HDMPC at the power tracking layer. The

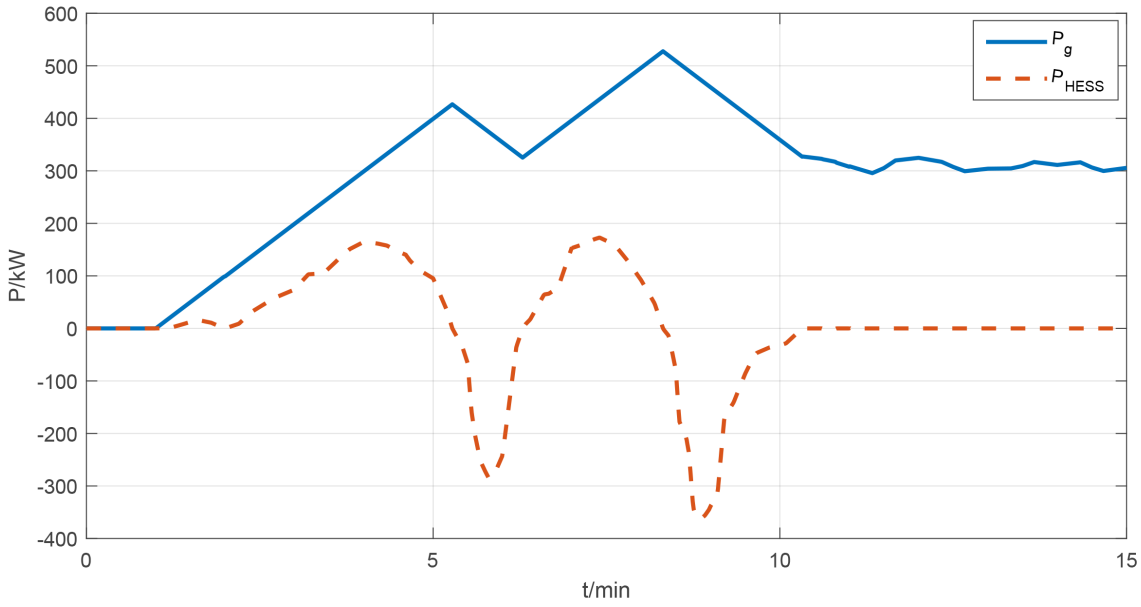

FIGURE 4. Power distribution results curve

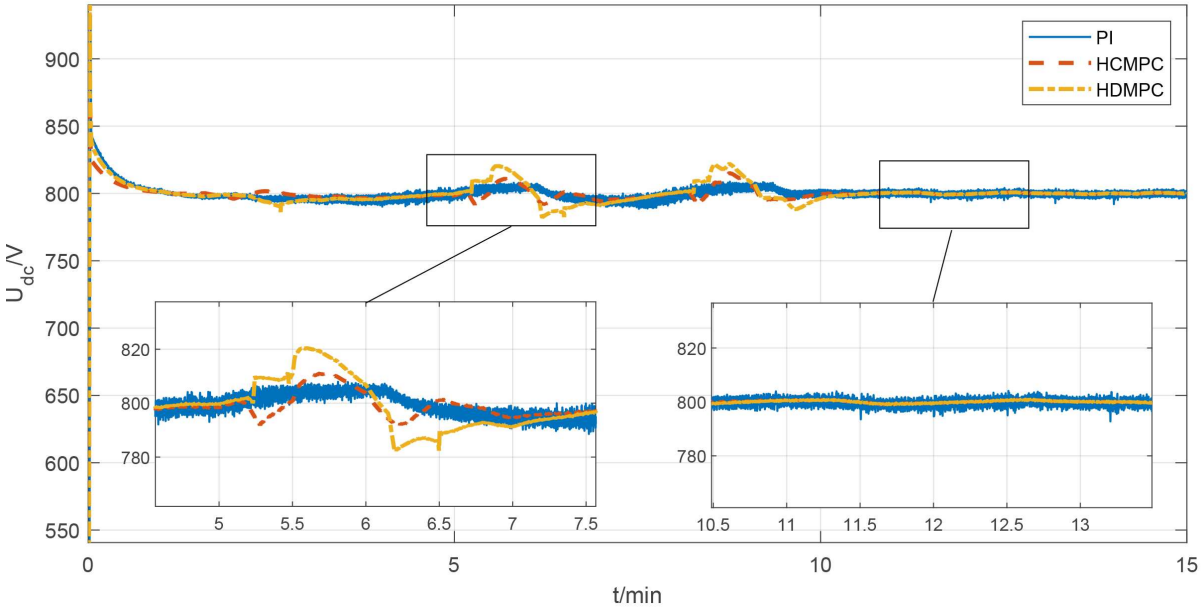

FIGURE 5. Comparison of DC bus voltage with PI and HCMPC

composition of its cost function J, the weight matrices Q_1, Q_2 and Q_3 and the choice of prediction and control horizon N are also consistent with the cost function (11) of DMPC in HDMPC. As the figure shown, the DC bus voltage has been stable at 800 V. HDMPC is less volatile than PI, and can be limited to 0.5 V, while PI is always about 2 V above and below. Both the proposed HDMPC and HCMPC can meet the load requirements quickly and stably. Compared with HCMPC, HDMPC has slightly larger fluctuations. However, HDMPC has less computational burden for the same DC microgrid system and predictive/control horizon. Under the same 1 s simulation time, the calculation time of HCMPC is 132 s, while the calculation time of each subsystem in HDMPC is 44 s. So with achieving similar performance as centralized control, distributed control

can decompose the large-scale online optimization problem into multiple small-scale optimization problems, which greatly reduces the computational burden.

From Figure 6, we can see that the delayed compensation is able to overcome the overshoot faster and bring the voltage to the rated value faster. To better compare the effect of voltage stability with and without delay compensation, we compare the voltage error convergence curves for the two different controls, as shown in Figure 7. In the figure we can see that the HDMPC with delay compensation converges to a smaller voltage error control than the normal HDMPC controller. To illustrate more directly the advantage of the algorithm in maintaining bus voltage stability, we introduce mean squared error (MSE), mean absolute error (MAE) and root mean square error (RMSE) for voltage error for comparison. The voltage error data are shown in Table 2.

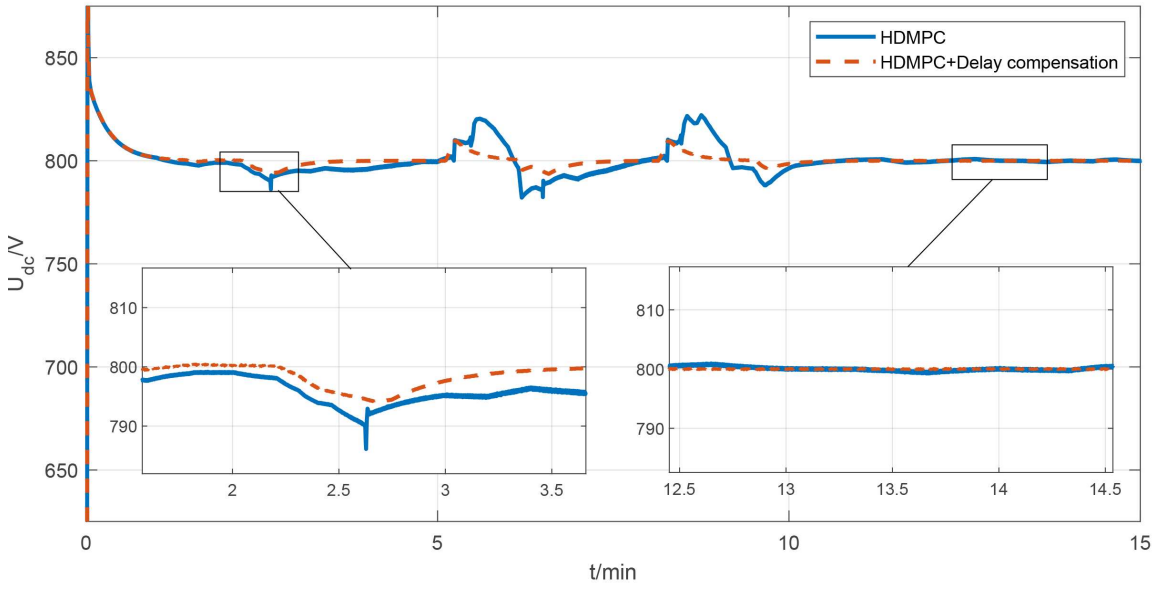

FIGURE 6. Effect of delayed compensation on DC bus voltage in HDMPC

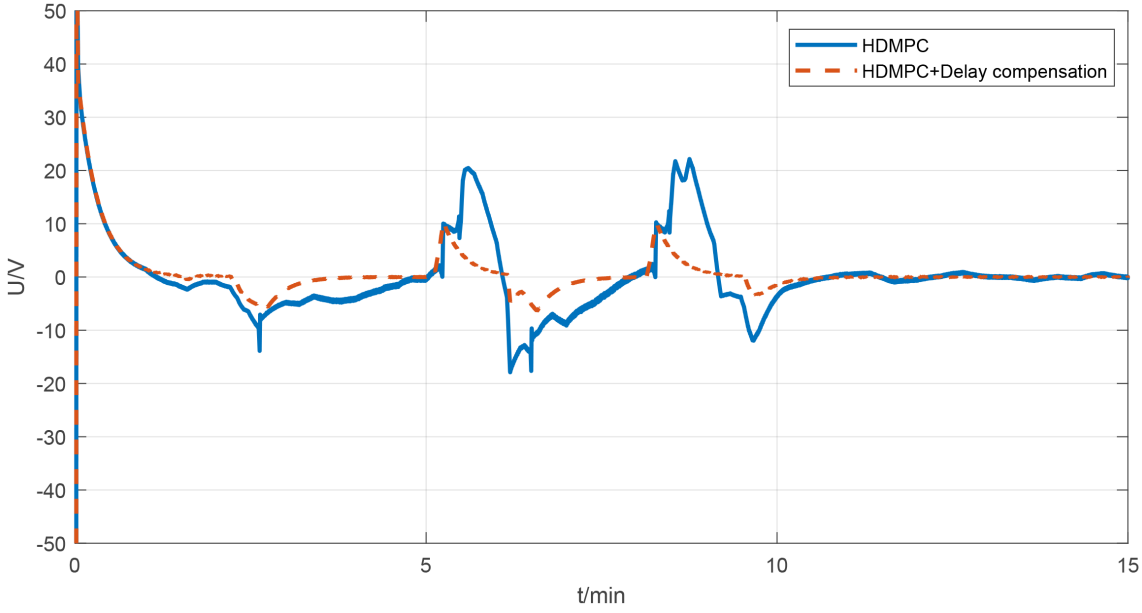

FIGURE 7. Voltage error convergence curves

TABLE 2. Voltage error data

Voltage error index	HDMPC	HDMPC+Delay compensation
MSE	391.17	355.13
MAE	5.08	2.43
RMSE	19.78	18.84

From Table 2, we can see that HDMPC with delay compensation performs better in various error parameters. Here we are able to see that the HDMPC proposed in this paper has a good control effect on the bus voltage of the DC microgrid.

Figure 8 shows that the output power can track the reference power quickly and accurately in the whole process, the average value of tracking error during the period is 0.48 kW, and the maximum value of error is 9.6 kW in about $t = 9.5$ min. When reaching the steady state, the power fluctuation is only within 0.3 kW.

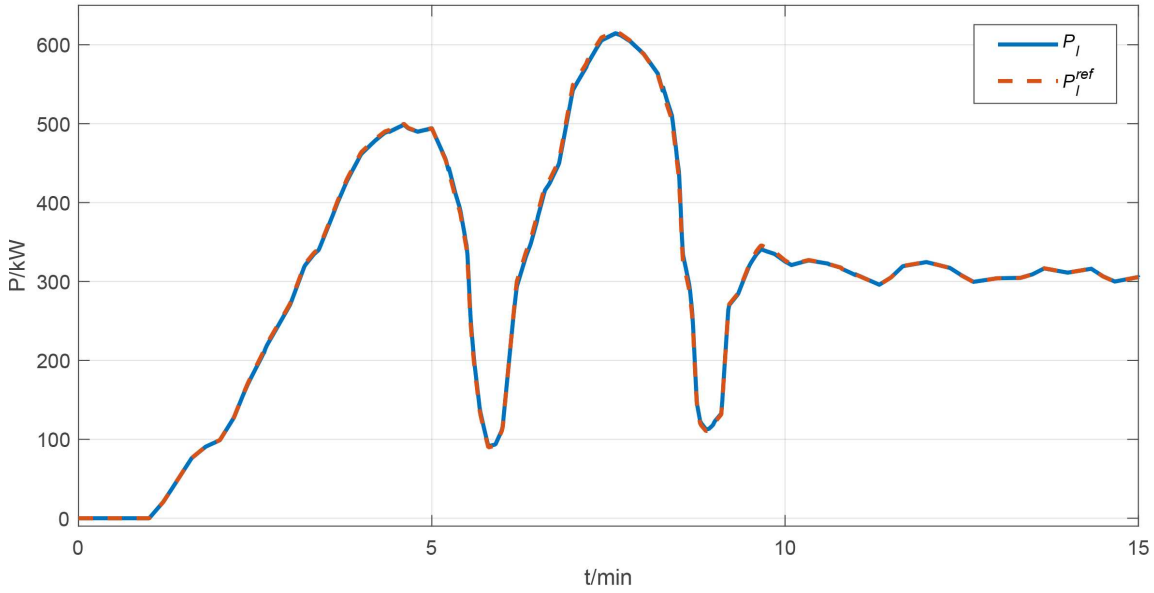

FIGURE 8. Power tracking curve

Figure 9 shows the respective SOC change curves of two batteries and two supercapacitors with different initial SOC values during operation. According to the optimization principle, the battery with higher SOC takes more power distribution in energy coordination. For battery#1, its SOC value dropped from 80% at the beginning to 78.9% at $t = 15$ min, the SOC drop value is $\Delta q_{b1} = 1.1\%$, while battery#2 only dropped from 60% to 59.6% and its $\Delta q_{b2} = 0.4\%$. Similarly, supercapacitor#1 dropped from 80% to 77.7%, the SOC drop value is $\Delta q_{c1} = 2.3\%$, while supercapacitor#2 with lower SOC value dropped from 60% to 58.9% and its $\Delta q_{c2} = 1.1\%$. It can be seen that battery#1 and supercapacitor#1 take up more output power in the whole HESS.

In MPC, although the system performance depends on a sufficiently accurate system model, its receding horizon characteristics make MPC have certain robustness. To show the robustness of the HDMPC strategy proposed in the case of changing system parameters, we changed some of the parameters in Table 1 and their voltage curves are shown in Figure 10. Curve 1 shows the case of changing the filter capacitor value $C_{bi} = 1000$ μF, Curve 2 shows the case of changing the inductance value $L_{bi} = L_{ci} = 3$ mH and Curve 3 shows that the battery voltage U_{bi} decreases to 400 V due to low SOC level.

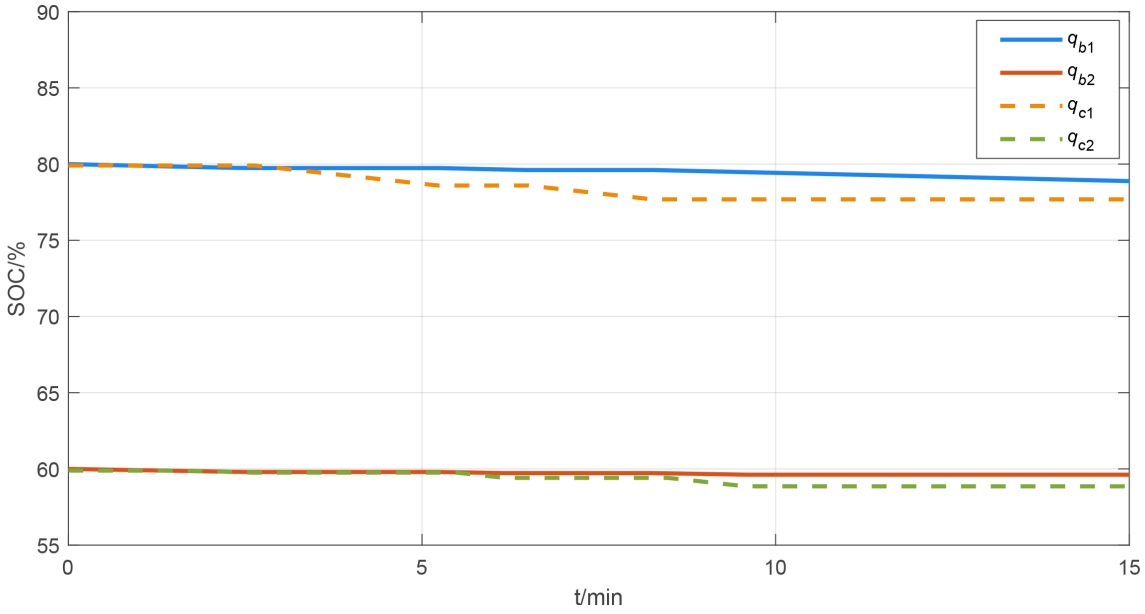

FIGURE 9. The SOC curve of each unit

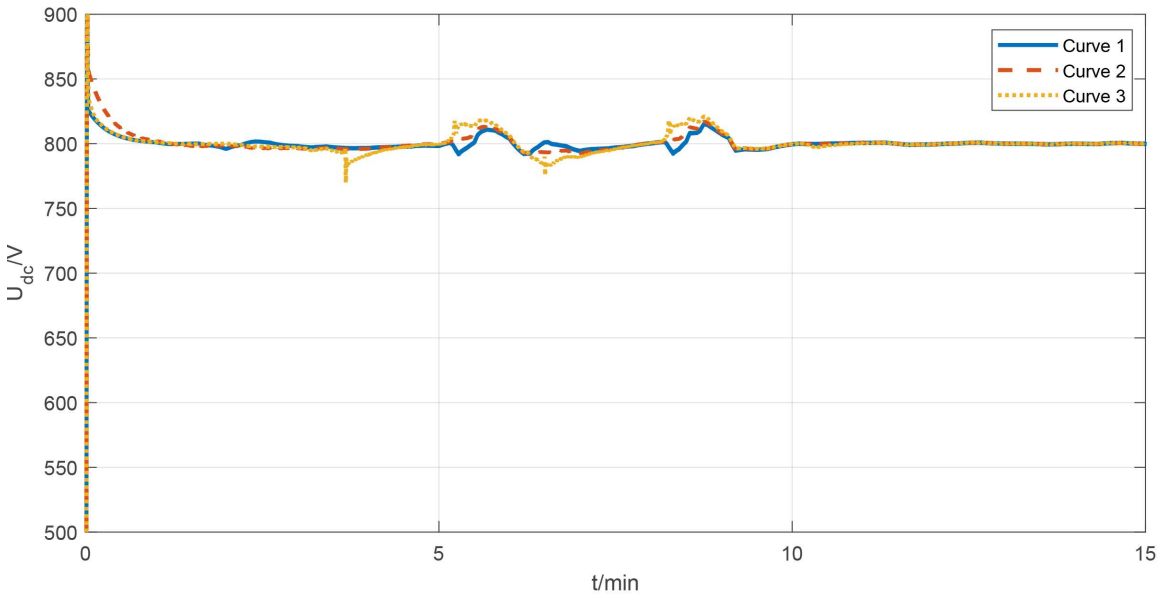

FIGURE 10. The DC bus voltage of different settings of DC microgrid

As shown in Figure 10, under different changes of system parameters, the model mismatch is caused by the parameter changes, so its bus voltage shows a large fluctuation, but it is still stable at the set value of about 800 V and the fluctuation magnitude does not change much. Thus, it can be concluded that the HDMPC strategy proposed in this paper can maintain the robustness of the system well under the change of system parameters.

5. **Conclusions.** An HDMPC approach is proposed for microgrids with multiple HESSs. The method considers the power scheduling of various sources in the upper layer, which solves the optimization problem in a distributed way using ADMM. The one-step delay compensation is further considered due to the computational burden caused during the iterations. The upper layer determines the power references for the lower layer, which

employs the FCS-MPC to address the power tracking problem. Simulations are carried out to verify the proposed approach. It shows that HDMPC enables the HESS system to operate stably, keeping the DC bus voltage around the load value given load fluctuations. Moreover, comparisons between the proposed method and some existing ones are given. The advantages of the proposed HDMPC approach include quick responses and smaller ripples. Our future work is to extend the results to multiple HESSs with parameter uncertainties and exogenous disturbances.

Acknowledgment. This work was supported in part by the National Natural Science Foundation of China under Grants 61903158, 61973140 and 62222307.

REFERENCES

[1] L. Che, M. Shahidehpour, A. Alabdulwahab et al., Hierarchical coordination of a community microgrid with AC and DC microgrids, *IEEE Transactions on Smart Grid*, vol.6, no.6, pp.3042-3051, 2015.

[2] L. Xu and D. Chen, Control and operation of a DC microgrid with variable generation and energy storage, *IEEE Transactions on Power Delivery*, vol.26, no.4, pp.2513-2522, 2011.

[3] A. El-Shahat and S. Sumaiya, DC-microgrid system design, control, and analysis, *Electronics*, vol.8, no.2, 124, 2019.

[4] W. Yan, L. Sheng, D. Xu et al., H_∞ robust load frequency control for multi-area interconnected power system with hybrid energy storage system, *Applied Sciences*, vol.8, no.10, 1748, 2018.

[5] W. Yang, D. Yu, D. Xu et al., Observer-based sliding mode FTC for multi-area interconnected power systems against hybrid energy storage faults, *Energies*, vol.12, no.14, 2819, 2019.

[6] R. Böhm, M. Steglich, C. Rehtanz et al., Control of a hybrid energy storage system for a hybrid compensation system, *Chemical Engineering & Technology*, vol.42, no.9, pp.1879-1885, 2019.

[7] J. Xiao, P. Wang and L. Setyawan, Hierarchical control of hybrid energy storage system in DC microgrids, *IEEE Transactions on Industrial Electronics*, vol.62, no.8, pp.4915-4924, 2015.

[8] R. Hemmati and H. Saboori, Emergence of hybrid energy storage systems in renewable energy and transport applications – A review, *Renewable and Sustainable Energy Reviews*, vol.65, pp.11-23, 2016.

[9] D. Xu, J. Liu, X. G. Yan et al., A novel adaptive neural network constrained control for a multi-area interconnected power system with hybrid energy storage, *IEEE Transactions on Industrial Electronics*, vol.65, no.8, pp.6625-6634, 2017.

[10] D. Xu, Q. Liu, W. Yan et al., Adaptive terminal sliding mode control for hybrid energy storage systems of fuel cell, battery and supercapacitor, *IEEE Access*, vol.7, pp.29295-29303, 2019.

[11] X. Song, J. Deng, D. Xu et al., Generic model control for hybrid energy storage system in electric vehicles, *IECON 2017 – The 43rd Annual Conference of the IEEE Industrial Electronics Society*, pp.7151-7156, 2017.

[12] S. Chen, Q. Yang, J. Zhou et al., A model predictive control method for hybrid energy storage systems, *CSEE Journal of Power and Energy Systems*, vol.7, no.2, pp.329-338, 2020.

[13] T. S. Babu, K. R. Vasudevan, V. K. Ramachandaramurthy et al., A comprehensive review of hybrid energy storage systems: Converter topologies, control strategies and future prospects, *IEEE Access*, vol.8, pp.148702-148721, 2020.

[14] Q. Liu, D. Xu, B. Jiang and Y. Ren, Prescribed-performance-based adaptive control for hybrid energy storage systems of battery and supercapacitor in electric vehicles, *International Journal of Innovative Computing, Information and Control*, vol.16, no.2, pp.571-583, 2020.

[15] W. Zhang, Y. Xia, D. Xu et al., Command-filtered backstepping controller for DC microgrid with hybrid energy storage devices, *2020 IEEE 9th Data Driven Control and Learning Systems Conference (DDCLS)*, pp.865-869, 2020.

[16] S. M. Tan, B. Wang, U. Manandhar et al., Model predictive control for hybrid energy storage system using single-inductor dual-input single-output converter, *2018 IEEE Innovative Smart Grid Technologies-Asia (ISGT Asia)*, pp.97-102, 2018.

[17] Z. Song, H. Hofmann, J. Li et al., Optimization for a hybrid energy storage system in electric vehicles using dynamic programing approach, *Applied Energy*, vol.139, pp.151-162, 2015.

[18] X. Wan and J. Wu, Distributed hierarchical control for islanded microgrids based on adjustable power consensus, *Electronics*, vol.11, no.3, 324, 2022.

[19] C. A. Hans, P. Braun, J. Raisch et al., Hierarchical distributed model predictive control of interconnected microgrids, *IEEE Transactions on Sustainable Energy*, vol.10, no.1, pp.407-416, 2018.
[20] Z. Zhang, D. Yue and C. X. Dou, DMPC-based coordinated voltage control for integrated hybrid energy system, *IEEE Transactions on Industrial Informatics*, vol.17, no.10, pp.6786-6797, 2020.
[21] J. Ni and P. Shi, Fixed-time event-triggered distributed controller for secondary voltage restoration in microgrid, *ICIC Express Letters*, vol.16, no.6, pp.595-604, 2022.
[22] E. Mojica-Nava, C. A. Macana and N. Quijano, Dynamic population games for optimal dispatch on hierarchical microgrid control, *IEEE Transactions on Systems, Man, and Cybernetics: Systems*, vol.44, no.3, pp.306-317, 2013.
[23] R. Scattolini, Architectures for distributed and hierarchical model predictive control – A review, *Journal of Process Control*, vol.19, no.5, pp.723-731, 2009.
[24] D. Xu, A. Xu, C. Yang et al., A novel double-quadrant SOC consistent adaptive droop control in DC microgrids, *IEEE Transactions on Circuits and Systems II: Express Briefs*, vol.67, no.10, pp.2034-2038, 2019.
[25] H. Wu, C. Wang, Y. Zhou, W. Xie and C. Chen, A method for local analysis of electric energy monitoring data, *International Journal of Innovative Computing, Information and Control*, vol.18, no.1, pp.105-119, 2022.
[26] Q. Yang, J. Zhou, X. Chen et al., Distributed MPC-based secondary control for energy storage systems in a DC microgrid, *IEEE Transactions on Power Systems*, vol.36, no.6, pp.5633-5644, 2021.
[27] S. Batiyah, R. Sharma, S. Abdelwahed et al., An MPC-based power management of standalone DC microgrid with energy storage, *International Journal of Electrical Power & Energy Systems*, vol.120, 105949, 2020.
[28] M. Jami, Q. Shafiee, K. Eguchi and H. Bevrani, Stability and inertia response improvement of boost converters interlaced with constant power loads, *International Journal of Innovative Computing, Information and Control*, vol.16, no.2, pp.765-782, 2020.
[29] K. Bi, Y. Liu, B. Tian et al., Analysis and design of an impedance source modular DC/DC converter for energy storage system, *2020 IEEE 9th International Power Electronics and Motion Control Conference (IPEMC2020-ECCE Asia)*, pp.1318-1323, 2020.
[30] Z. Jin, S. Liu, L. Jin et al., Model based robust predictive control of ship roll/yaw motions with input constraints, *Applied Sciences*, vol.10, no.10, 3377, 2020.
[31] L. K. Marepalli, K. Gajula and L. Herrera, Model predictive control for current sharing and voltage balancing in DC microgrids, *2021 IEEE Energy Conversion Congress and Exposition (ECCE)*, pp.1040-1045, 2021.
[32] W. Yang, A. Arystan, G. Hu, D. Xu, W. Zhang and Y. Xia, A novel multi-step finite-control-set model predictive control approach for permanent magnet synchronous motors, *International Journal of Innovative Computing, Information and Control*, vol.17, no.2, pp.425-441, 2021.
[33] S. Kouro, P. Cortés, R. Vargas et al., Model predictive control – A simple and powerful method to control power converters, *IEEE Transactions on Industrial Electronics*, vol.56, no.6, pp.1826-1838, 2008.
[34] B. Hredzak, V. G. Agelidis and M. Jang, A model predictive control system for a hybrid battery-ultracapacitor power source, *IEEE Transactions on Power Electronics*, vol.29, no.3, pp.1469-1479, 2013.
[35] S. Boyd, N. Parikh, E. Chu et al., Distributed optimization and statistical learning via the alternating direction method of multipliers, *Foundations and Trends® in Machine Learning*, vol.3, no.1, pp.1-122, 2011.

Author Biography

Weilin Yang received his B.Eng. degree in Machine Design & Manufacture and Their Automation from University of Science and Technology of China, Hefei, China, in 2009, and the Ph.D. degree in Mechanical Engineering from City University of Hong Kong, Hong Kong SAR in 2013.

He was a Postdoctoral Researcher at Masdar Institute of Science and Technology (now Khalifa University), Abu Dhabi, UAE, 2013-2016. He was a Research Engineer of General Electric (GE) Global Research, Shanghai, 2016-2017. He joined Jiangnan University in July 2017, where he is currently an Associate Professor. His research interests include modeling and control of energy systems, robust model predictive control, and dada-driven control.

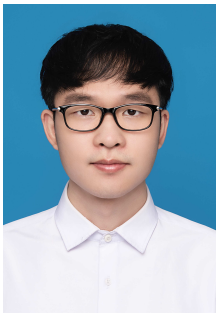

Chaonan Zhao received his B.Sc. degree in Electrical Engineering and Automation from Jiangnan University, China, in 2018. He is currently pursuing his M.Sc. degree in Electrical Engineering at Jiangnan University. His main research interests include hybrid energy storage technology and distributed model predictive control.

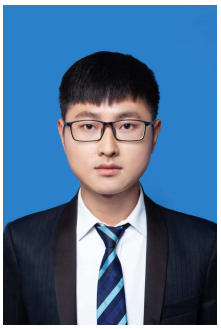

Guanyang Hu received the B.S. degree in Electrical Engineering and Automation from Linyi University and the M.S. degree in Electrical Engineering from Jiangnan University, in 2019 and 2022, respectively. At present, he is currently working toward the Ph.D. degree in Control Science and Engineering at Jiangnan University. His research interests include electric machine drives and distributed model predictive control.

Dezhi Xu received the Ph.D. degree in Control Theory and Control Engineering from Nanjing University of Aeronautics and Astronautics, China, in 2013.

He was a Visiting Fellow with the Department of Biomedical Engineering, City University of Hong Kong, Hong Kong, from 2018 to 2019. He is currently a Professor and Doctoral Supervisor with the Jiangnan University. His current research interests include data-driven control, fault diagnosis and fault-tolerant control, multi-agent systems and CPSs, technologies of renewable energy, motor control, and smart grid. Prof. Xu was a recipient of the First Class Prize of Science and Technology Progression from the China General Chamber of Commerce in 2016, and the Best Young Scholar of Jiangnan University in 2022 for his research results. He is currently a Guest Editor or an Editorial Board Member for a number of journals, such as the *International Journal of Innovative Computing, Information and Control*, the *Electric Power*, the *Zhejiang Electric Power*, the *Electrotechnical Application*, and the *Electrical Engineering*. He is a Committee Member of the Association of Energy Internet, and Trusted Control in Chinese Association of Automation (CAA), and the Energy Storage in China Renewable Energy Society (CRES).

Tinglong Pan received his B.Eng. degree in Industrial Automation from China University of Mining and Technology, Xuzhou, China, in 1999, and the Ph.D. degree in Power Electronics and Power Drive from China University of Mining and Technology, Xuzhou, China, in 2004.

He is currently a Professor at Jiangnan University, where his research interests include microgrid control technology, power conversion technology, power drive system and its intelligent control technology.